NUCLEAR THEORY, Vol. 38 (2019)
eds. M. Gaidarov, N. Minkov, Heron Press, Sofia

Isotopic and Isotonic Evolution of the Symmetry Energy and Skins of Mirror Nuclei

M.K. Gaidarov[1], **I. Moumene**[2], **A.N. Antonov**[1], **D.N. Kadrev**[1], **P. Sarriguren**[3], **E. Moya de Guerra**[4]

[1]Institute for Nuclear Research and Nuclear Energy, Bulgarian Academy of Sciences, Sofia 1784, Bulgaria

[2]High Energy Physics and Astrophysics Laboratory, Faculty of Science Semlalia, Cadi Ayyad University, P.O.B. 2390, Marrakesh, Morocco

[3]Instituto de Estructura de la Materia, IEM-CSIC, Serrano 123, E-28006 Madrid, Spain

[4]Grupo de Física Nuclear, Departamento de Física Atómica, Molecular y Nuclear, Facultad de Ciencias Físicas, Universidad Complutense de Madrid, E-28040 Madrid, Spain

Abstract. The knowledge of the neutron skin is important for nuclear physics and astrophysics, but its experimental determination faces many challenges. We calculate the neutron skin of a nucleus by using the possibility to relate it with the difference between the proton radii of the corresponding mirror nuclei as an alternative way. The calculations are based on the Hartree-Fock-Bogoliubov method by using the cylindrical transformed deformed harmonic-oscillator basis. Predictions for proton skins are also made for several mirror pairs in the middle mass range. The correlation between the thickness of the neutron skin and the characteristics related with the density dependence of the nuclear symmetry energy is investigated for Ni isotopic chain with mass number $A = 48 - 60$ and the respective mirror nuclei. These quantities are calculated within the coherent density fluctuation model using Brueckner and Skyrme energy-density functionals for isospin asymmetric nuclear matter with two Skyrme-type effective interactions, SkM* and SLy4. Results are also presented for the symmetry energy as a function of A for a family of mirror pairs from selected chains of nuclei with $Z = 20$, $N = 14$, and $N = 50$. The evolution curves show a similar behavior crossing at the double-magic nucleus in each chain and a smooth growing deviation when $N \neq Z$ starts. Comparison of our results for the radii and skins with those from the calculations based on high-precision chiral forces is made.

1 Introduction

The neutron skin thickness has been identified as a strong isovector indicator [1]. The knowledge of the skin thickness gives more insight into the properties of neutron-rich nuclei and neutron stars, and the equation of state (EOS)

of asymmetric nuclear matter (ANM). Immediate determination of the neutron skin thickness usually involves the precise measurement of the root mean square (rms) radii of both charge and mass distributions. Electron-nucleus scattering has proven to be an excellent tool for the study of nuclear structure. In particular, it has accumulated much reliable information on charge density distributions of stable nuclei. Therefore, it is believed that the new facilities in GSI [2], ISOLDE-CERN [3], and RIKEN [4] will provide a good opportunity to study the charge density, and consequently the proton density distribution, of unstable nuclei by elastic electron scattering. In RIKEN-SCRIT the first elastic electron scattering experiment on ^{132}Xe has already been performed [5]. Unfortunately, a measurement of the neutron density distributions to a precision and detail comparable to that of the proton one is hardly possible. It turned out that to get information on the neutron skin thickness one needs data obtained with probes having different sensitivities to the proton and neutron distributions.

The model-independent measurement of parity-violating asymmetry [6] (which is sensitive to the neutron distribution) in the elastic scattering of polarized electrons from ^{208}Pb at JLAB within the PREX Collaboration [7,8] has provided the first electroweak observation of the neutron skin thickness $0.33^{+0.16}_{-0.18}$ fm in ^{208}Pb (see also [9] for more discussion). A PREX-II experiment has been approved that is expected to reach the 0.06 fm sensitivity in the neutron radius of ^{208}Pb, and parity-violating experiments are planned for ^{48}Ca nucleus [10].

It has been shown in Ref. [11] that in the case of a perfect charge symmetry the neutron skin in a given nucleus can be obtained from the proton radii of mirror nuclei. Therefore, besides the planned JLAB experiment, measurements of mirror charge radii could be an alternative with a competitive precision. The only step after measuring the charge rms radii is to apply the relativistic and finite size corrections to deduce the point-proton rms radii. The correlations discussed in Ref. [11] between the neutron skin and the difference of the proton radii are determined for a particular mirror pair. This was realized by constructing 48 Skyrme functionals to predict different skins of ^{208}Pb within a chosen range. Moreover, it was also shown that the differences in the charge radii of mirror nuclei is proportional to the slope of the symmetry energy L at saturation density, even in the presence of Coulomb corrections. The same findings have been confirmed in an approach based on a set of relativistic energy density functionals (EDFs) spanning a wide region of values of L [12]. In a recent work [13] Sammarruca has applied an isospin-asymmetric EOS derived microscopically from high-precision chiral few-nucleon interactions to study these correlations for a family of mirror pairs, in contrast to the consideration presented in [11].

In the present paper we aim to investigate the relations between the quantities defined above among isotopic and isotonic chains with different masses. We focus on nuclei in the mass region $A = 48 - 60$, in which the Ni isotopes and respective mirror nuclei are studied. Additionally to the results presented in [13], we search for possible correlation between the neutron skin thickness and the EOS parameters (symmetry energy, pressure, asymmetric compressibility),

but for the mirrors of Ni isotopes, in a similar way done in Refs. [9, 14, 15], where such correlations have been validated. We calculate the proton skins of Argon isotopes ($A = 32 - 40$) and predictions for them are made, in comparison with the empirical data [16] and the microscopic results of Sammarruca [13]. Also, we pay particular attention to the $Z = 20$ isotopic chain, including ^{48}Ca, inspired by the new experiment on this nucleus (CREX). Finally, we inspect the relation between the neutron skin and the difference of the proton radii of the corresponding mirror nuclei for the $N = 14$ and $N = 50$ isotonic chains. The nuclear densities and radii are calculated within a self-consistent Hartree-Fock-Bogoliubov (HFB) method by using the cylindrical transformed deformed harmonic-oscillator basis (HFBTHO) [17, 18] that has been adopted previously in Refs. [19, 20]. The results for the symmetry energy and characteristics related with its density dependence in these nuclei are obtained in the CDFM framework [21, 22] by use of Brueckner and Skyrme EDFs for infinite nuclear matter with two Skyrme-type effective interactions: SLy4 and SkM*.

2 Symmetry of Mirror Nuclei

The definition of the neutron- and proton-skin thicknesses are, correspondingly:

$$\Delta R_n = R_n(Z,N) - R_p(Z,N), \tag{1}$$

and

$$\Delta R_p = R_p(Z,N) - R_n(Z,N), \tag{2}$$

As can be seen

$$\Delta R_n = -\Delta R_p. \tag{3}$$

Under the assumption of exact charge symmetry, the neutron radius of a given nucleus is identical to the proton radius of its mirror nucleus:

$$R_n(Z,N) = R_p(N,Z). \tag{4}$$

Let us introduce the following difference of the proton radii of a given nucleus and its mirror one:

$$\Delta R_{\text{mirr}} = R_p(N,Z) - R_p(Z,N). \tag{5}$$

Thus, in the case of the exact charge symmetry, using Eq. (4) in Eq. (1), one can obtain the equality of ΔR_n and ΔR_{mirr}:

$$\Delta R_n = R_p(N,Z) - R_p(Z,N) = \Delta R_{\text{mirr}}. \tag{6}$$

3 Brief Review of the Theoretical Scheme

Near the saturation density ρ_0 the symmetry energy for ANM, $S^{ANM}(\rho)$, can be expanded as

$$\begin{aligned} S^{ANM}(\rho) &= \frac{1}{2}\left.\frac{\partial^2 E(\rho,\delta)}{\partial\delta^2}\right|_{\delta=0} \\ &= a_4 + \frac{p_0^{ANM}}{\rho_0^2}(\rho-\rho_0) + \frac{\Delta K^{ANM}}{18\rho_0^2}(\rho-\rho_0)^2 + \cdots . \end{aligned} \quad (7)$$

The parameter a_4 is the symmetry energy at equilibrium ($\rho=\rho_0$). The pressure p_0^{ANM}

$$p_0^{ANM} = \rho_0^2 \left.\frac{\partial S^{ANM}}{\partial\rho}\right|_{\rho=\rho_0} \quad (8)$$

and the curvature ΔK^{ANM}

$$\Delta K^{ANM} = 9\rho_0^2 \left.\frac{\partial^2 S^{ANM}}{\partial\rho^2}\right|_{\rho=\rho_0} \quad (9)$$

of the nuclear symmetry energy at ρ_0 govern its density dependence and thus provide important information on the properties of the nuclear symmetry energy at both high and low densities. The widely used "slope" parameter L^{ANM} is related to the pressure p_0^{ANM} [Eq. (8)] by

$$L^{ANM} = \frac{3p_0^{ANM}}{\rho_0}. \quad (10)$$

Our basic assumption within the CDFM is that the symmetry energy, the slope and the curvature for finite nuclei can be defined weighting these quantities for nuclear matter by means of the weight function $|\mathcal{F}(x)|^2$ given below. Following the CDFM scheme, the symmetry energy, the slope and the curvature for finite nuclei have the following forms (see, for instance, Ref. [14]):

$$S = \int_0^\infty dx|\mathcal{F}(x)|^2 S^{ANM}(x), \quad (11)$$

$$p_0 = \int_0^\infty dx|\mathcal{F}(x)|^2 p_0^{ANM}(x), \quad (12)$$

$$\Delta K = \int_0^\infty dx|\mathcal{F}(x)|^2 \Delta K^{ANM}(x). \quad (13)$$

Analytical expressions for the nuclear matter quantities $S^{ANM}(x)$, $p_0^{ANM}(x)$, and $\Delta K^{ANM}(x)$ [Eqs. (11)-(13)] derived on the basis of Brueckner EDF can be found in Ref. [14]. As it was mentioned before, results for the isotopic and

isotonic evolution of the symmetry energy obtained also by Skyrme EDF will be presented.

We adopt a convenient approach to the weight function $|\mathcal{F}(x)|^2$ proposed in Refs. [21, 22]. In the case of monotonically decreasing local densities (*i.e.* for $d\rho(r)/dr \leq 0$), the latter can be obtained by means of a known density distribution $\rho(r)$ for a given nucleus:

$$|\mathcal{F}(x)|^2 = -\frac{1}{\rho_0(x)} \left.\frac{d\rho(r)}{dr}\right|_{r=x}. \tag{14}$$

The normalization of the weight function is:

$$\int_0^\infty dx|\mathcal{F}(x)|^2 = 1. \tag{15}$$

As far as the densities and the rms radii of the mirror nuclei are concerned, they have been obtained within the Skyrme HFB method [17, 18]. The HFBTHO code solves the nuclear Skyrme HFB problem by using the cylindrical transformed deformed harmonic-oscillator basis by implementing the finite temperature formalism for the HFB method. In our case we use densities at zero temperature. In HFBTHO, the direct term of the Coulomb potential to the total energy is taken into account.

4 Results and Discussion

We show first in Table 1 the results for the rms radii and proton skins predictions for $Z = 10$ and $Z = 18$ isotopic chains including neutron-deficient even-even isotopes in each chain. It can be seen that the proton skins of the presented nuclei are quite large. Second, there is a very good agreement of the proton skin values

Table 1. Neutron (R_n), proton (R_p), matter (R_m), and charge (R_c) rms radii (in fm) calculated with SLy4 Skyrme force for $Z = 10$ and $Z = 18$ isotopic chains. The proton skins ΔR_p (in fm) are also shown in comparison with the results obtained in Ref. [13].

Nucleus	Z	N	R_n	R_p	R_m	R_c	ΔR_p	ΔR_p [13]
^{16}Ne	10	6	2.51	2.89	2.76	3.00	0.378	0.422
^{18}Ne		8	2.67	2.85	2.77	2.96	0.175	0.186
^{20}Ne		10	2.81	2.84	2.82	2.95	0.030	0.032
^{30}Ar	18	12	3.00	3.32	3.20	3.42	0.323	0.352
^{32}Ar		14	3.07	3.28	3.19	3.38	0.216	0.225
^{34}Ar		16	3.17	3.29	3.23	3.39	0.123	0.127
^{36}Ar		18	3.26	3.31	3.29	3.40	0.050	0.046

Table 2. Predicted proton skins ΔR_p [Eq. (2)] (in fm) for several $Z = 10$ and $Z = 18$ nuclei (columns 1 and 2), neutron skins ΔR_n [Eq. (1)] (in fm) of the corresponding mirror nuclei (columns 3 and 4), and $\Delta R_{\rm mirr}$ [Eq. (6)] (in fm) (column 5) calculated with SkM* Skyrme force.

Nucleus	ΔR_p	Mirror Nucleus	ΔR_n	$\Delta R_{\rm mirr}$
^{16}Ne	0.366	^{16}C	0.308	-0.360
^{18}Ne	0.160	^{18}O	0.111	-0.147
^{30}Ar	0.327	^{30}Mg	0.238	-0.308
^{32}Ar	0.222	^{32}Si	0.136	-0.188
^{34}Ar	0.128	^{34}S	0.041	-0.088

derived from the HFBTHO code with the proton skins obtained in Ref. [13] on the base of EOS with high-precision chiral forces.

Table 2 illustrates the proton skins of several neutron-deficient isotopes with less neutrons than those given in Table 1 together with the neutron skin thickness of the corresponding mirror nuclei and the proton radii difference of the mirror pair $\Delta R_{\rm mirr}$. Indeed, the neutron skins are smaller than proton skins for comparable values of proton-neutron asymmetry.

Next, we show in Figure 1 the HFB predictions for the proton skins of Argon isotopes with $A = 30 - 36$. They are compared with the theoretical predictions from [13] for a more extended mass region $A = 29 - 40$ and experimental

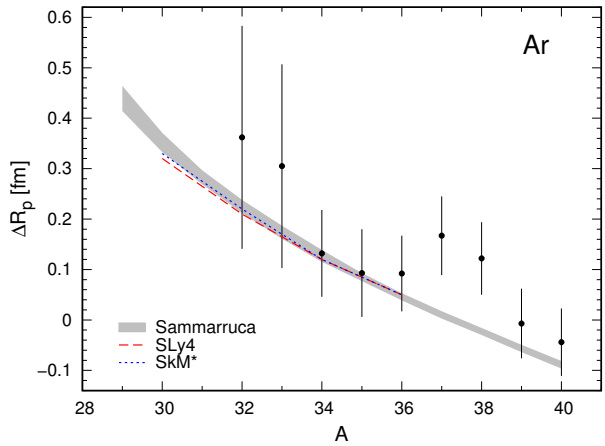

Figure 1. Predicted proton skins of Ar isotopes as a function of the mass number A. The results calculated with SLy4 and SkM* Skyrme interactions are given by red dashed and blue dotted lines, respectively. The gray band represents the result of F. Sammarruca [13] and the experimental data points are from Ozawa *et al.* [16].

proton skin thicknesses for isotopes $^{32-40}$Ar deduced from the interaction cross sections of $^{31-40}$Ar on carbon target [16]. In spite of the large errors of the empirical data, the predictions of both theoretical methods describe reasonably well their trend, namely the monotonic decrease of the proton skin with increasing of the neutron number N in a given isotopic chain. Actually, the data in Figure 1 cover a range of N that includes the magic number $N = 20$, but an enhancement of the proton skin is seen earlier at $N = 19$. More detailed consideration of the Ar isotopes around $A = 38$ is necessary to give a clear answer on the role of the shell effects on the behavior of the proton skin data in this mass region.

The relation between the neutron skin ΔR_n and the proton radii difference of the mirror pair $\Delta R_{\rm mirr}$ as defined in Eq. (6) is presented in Figure 2 on the examples of $Z = 28$ isotopic chain and two isotonic chains with $N = 14$ and $N = 50$. In all three cases a linear relation between these characteristics is observed. Note that the results are obtained in the presence of Coulomb effects. Similar linear relations are shown in Ref. [13] for the $N = 28$, $Z = 10$, and $Z = 20$ chains confirming an unique relation between ΔR_n and $\Delta R_{\rm mirr}$ regardless Z and N. Also, both Skyrme interactions provide similar results.

In what follows, we show results for the symmetry energy S obtained within the CDFM using first the Brueckner EDF for the symmetry energy in infinite nu-

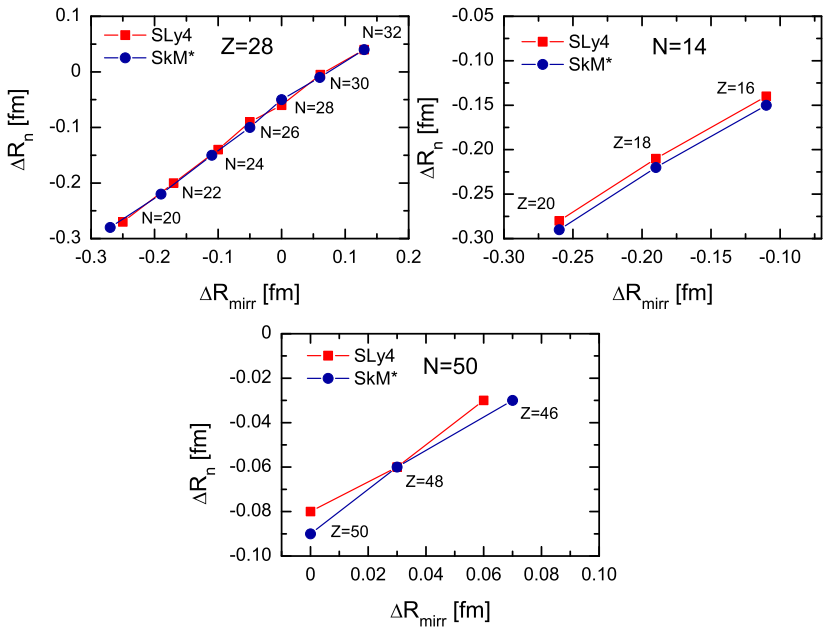

Figure 2. Relation between the neutron skin ΔR_n and $\Delta R_{\rm mirr}$ [Eq. (6)] for the $Z = 28$ isotopic chain and N=14 and N=50 isotonic chains. The results with SLy4 and SkM* Skyrme forces are given by red (with squares) and blue (with dots) lines, respectively.

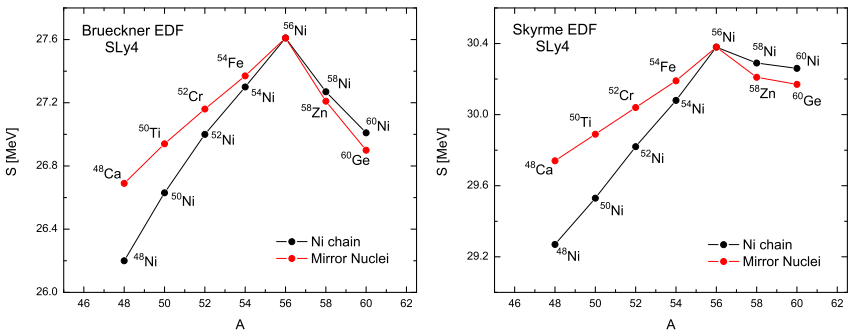

Figure 3. The symmetry energy S as a function of the mass number A for Ni isotopes (black line with circles) and their mirror nuclei (red line with circles) calculated with Brueckner (left panel) and Skyrme (right panel) EDFs in the case of SLy4 force.

clear matter S^{ANM} in Eq. (11), while the wight function $|\mathcal{F}(x)|^2$ is obtained using Eq. (14) by means of the density distribution within the Skyrme HFB method (the HFBTHO densities). Second, we calculate in the CDFM the symmetry en-

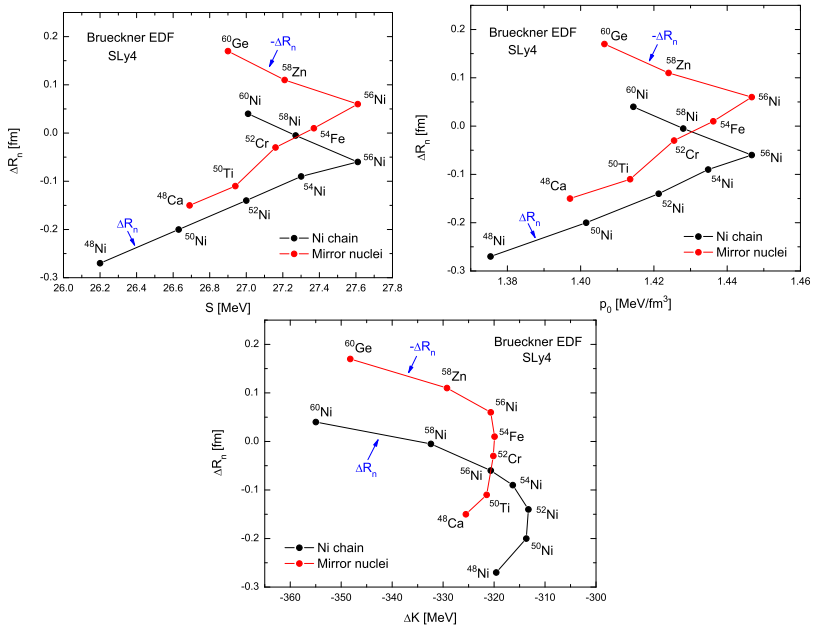

Figure 4. HFB neutron skin thickness ΔR_n for Ni isotopes (black line with circles) and corresponding proton skins for their mirror nuclei (red line with circles) as a function of the symmetry energy S, pressure p_0, and asymmetric compressibility ΔK calculated with Brueckner EDF and SLy4 force.

ergy S using also the Skyrme EDF. In this case there is a self-consistency between the way to obtain $|\mathcal{F}(x)|^2$ in the Skyrme HFB method and the use of the Skyrme EDF to obtain the symmetry energy.

The mass dependence of the symmetry energy S for the Ni isotopes ($Z = 28$) with $A = 48-60$ and their mirror nuclei by using the Brueckner and Skyrme EDFs with SLy4 force is presented in Figure 3. The behavior of the curves for the two functionals is similar and the values of S obtained with Skyrme EDF are larger in comparison with the corresponding values deduced with Brueckner EDF. An important result, which can be seen from Figure 3, is that the mirror nuclei demonstrate the same linear behavior like the evolution of the symmetry energy in Ni chain of heavier isotopes [14] containing an inflection point ("kink") at the double-magic ^{56}Ni nucleus. In addition, there is a small shift of

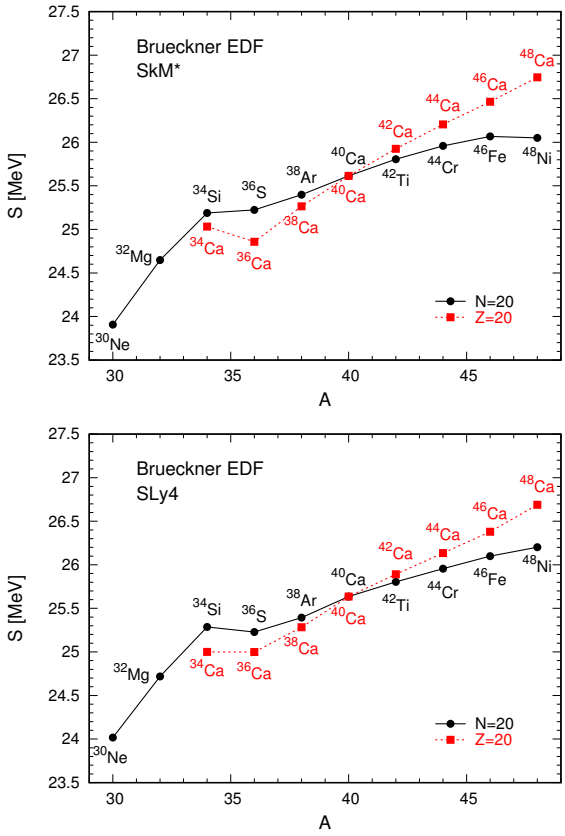

Figure 5. The symmetry energy S as a function of the mass number A for Ca isotopes (red line with squares) and their mirror nuclei (black line with circles) calculated with Brueckner EDF and SkM* (upper panel) and SLy4 (lower panel) forces.

the curve for mirror nuclei in respect with the Ni curve with a smooth growing deviation between them when $|N - Z|$ starts to increase.

An approximate linear correlation between ΔR_n and S for the same mirror pairs presented in Figure 3 is seen from Figure 4. The correlation between ΔR_n and p_0 is similar, while a less strong correlation between ΔR_n and ΔK is found. As in the symmetry-energy case, the behavior of the curves drawn in these plots shows the same tendency, namely, the inflection point transition at the double-magic ^{56}Ni nucleus.

Finally, in Figure 5 we display results on the isotopic evolution of the symmetry energy for the $Z = 20$ isotopes and the corresponding mirror nuclei. They are shown for the case of Brueckner EDF with both SkM* and SLy4 forces. In contrast to the Ni chain, no "kink" is observed, particularly at the double-magic ^{40}Ca nucleus. The corresponding mirror nuclei ($N = 20$ isotones) also reveal a linear behavior but with an inflection point transition at ^{34}S nucleus. The predicted double-magicity of ^{34}S is discussed in [23] but no unambiguous evidence is found.

5 Summary and Conclusions

The HFB method by using the cylindrical transformed deformed harmonic-oscillator basis has been applied to calculations of radii and skins for several mirror pairs in the middle mass range. The parameters of the EOS (S, p_0, ΔK) have been calculated for Ni isotopic chain with mass number $A = 48 - 60$, as well as for nuclei with $Z = 20$, $N = 14$, and $N = 50$ and their respective mirror nuclei using Brueckner and Skyrme EDFs for isospin asymmetric nuclear matter with two Skyrme-type forces, SkM* and SLy4, and the CDFM as a "bridge" from nuclear matter to finite nuclei.

The main results of the present study can be summarized, as follows:

i) The predicted proton skins are found quite large, larger than the neutron skins of the corresponding mirror nuclei. They compare reasonably well with available empirical data, for instance for Ar isotopes, that are also well described by chiral effective field theory-based EOS;

ii) The studied relation between the neutron skin ΔR_n and the difference between the proton radii $\Delta R_{\rm mirr}$ for a family of mirror pairs in the presence of Coulomb effects shows clearly a linear dependence. Thus, this could be an alternative way to explore neutron skins that challenges experimentalists to perform high-precision measurements of the charge radii of unstable neutron-rich isotopes;

iii) In the case of Ni isotopic chain and the respective mirror nuclei we found a strong correlation between the neutron (proton) skin thickness and the S and p_0 parameters of the EOS with a "kink" at double-magic ^{56}Ni, while the correlation with ΔK is less pronounced;

iv) The evolution of the symmetry energy S with the mass number A of nuclei from $Z = 20$, $Z = 28$, and $N = 50$ chains and their mirror nuclei

exhibits similar behavior. The curves cross in each chain at the double-magic nucleus (^{40}Ca, ^{56}Ni, ^{100}Sn) and start to deviate from each other with the increase of $|N - Z|$.

Acknowledgements

This work was partially supported by the Bulgarian National Science Fund under Contract No. KP-06-N38/1.

References

[1] P.-G. Reinhard and W. Nazarewicz, *Phys. Rev. C* **81** (2010) 051303.
[2] A.N. Antonov *et al.*, *Nucl. Instr. and Meth. in Phys. Res. A* **637** (2011) 60.
[3] R.F. Garcia Ruiz *et al. Nat. Phys.* **12** (2016) 594.
[4] T. Suda and M. Wakasugi, *Prog. Part. Nucl. Phys.* **55** (2005) 417.
[5] K. Tsukada *et al.*, *Phys. Rev. Lett.* **118** (2017) 262501.
[6] O. Moreno, P. Sarriguren, E. Moya de Guerra, J.M. Udias, T.W. Donnelly, and I. Sick, *Nucl. Phys. A* **828** (2009) 306.
[7] http://hallaweb.jlab.org/parity/prex.
[8] S. Abrahamyan *et al.*, *Phys. Rev. Lett.* **108** (2012) 112502.
[9] M.K. Gaidarov, A.N. Antonov, P. Sarriguren, and E. Moya de Guerra, *Phys. Rev. C* **85** (2012) 064319.
[10] C.J. Horowitz, K.S. Kumar, and R. Michaels, *Eur. Phys. J. A* **50** (2014) 48.
[11] B. Alex Brown, *Phys. Rev. Lett.* **119** (2017) 122502.
[12] Junjie Yang and J. Piekarewicz, *Phys. Rev. C* **97** (2018) 014314.
[13] F. Sammarruca, *Front. Phys.* **6:90** (2018).
[14] M.K. Gaidarov, A.N. Antonov, P. Sarriguren, and E. Moya de Guerra, *Phys. Rev. C* **84** (2011) 034316.
[15] M.K. Gaidarov, P. Sarriguren, A.N. Antonov, and E. Moya de Guerra, *Phys. Rev. C* **89** (2014) 064301.
[16] A. Ozawa, T. Baumann, L. Chulkov, D. Cortina, U. Datta, J. fernandez *et al.*, *Nucl. Phys. A* **709** (2002) 60.
[17] M.V. Stoitsov *et al.*, *Comput. Phys. Commun* **184** (2013) 1592.
[18] M. V. Stoitsov, J. Dobaczewski, W. Nazarewicz, and P. Ring, *Comput. Phys. Comm.* **167** (2005) 43.
[19] A. N. Antonov, D. N. Kadrev, M. K. Gaidarov, P. Sarriguren, and E. Moya de Guerra, *Phys. Rev. C* **95** (2017) 024314.
[20] A. N. Antonov, D. N. Kadrev, M. K. Gaidarov, P. Sarriguren, and E. Moya de Guerra, *Phys. Rev. C* **98** (2018) 054315.
[21] A.N. Antonov, V.A. Nikolaev, and I.Zh. Petkov, *Bulg. J. Phys.* **6** (1979) 151; *Z. Phys. A* **297** (1980) 257; *ibid* **304** (1982) 239; *Nuovo Cimento A* **86** (1985) 23; A.N. Antonov *et al.*, *ibid* **102** (1989) 1701; A.N. Antonov, D.N. Kadrev, and P.E. Hodgson, *Phys. Rev. C* **50** (1994) 164.
[22] A.N. Antonov, P.E. Hodgson, and I.Zh. Petkov, *Nucleon Momentum and Density Distributions in Nuclei*, Clarendon Press, Oxford (1988); *Nucleon Correlations in Nuclei*, Springer-Verlag, Berlin-Heidelberg-New York (1993).
[23] I. Angeli and K. Marinova, *J. Phys. G* **42** (2015) 055108.